Three-dimension dynamic simulation of thin epoxy-resin plate and comparison with experiment

Hao Chen[1,*] **, Tomoo Okinaka**[2]

[1] Key Laboratory of Earthquake Engineering and Engineering Vibration,
Institute of Engineering Mechanics, CEA, Sanhe, 065201, China
[2] Kinki University, Higashi-Osaka, 577-8502, Japan
* Corresponding author: chenhao@iem.ac.cn

Abstract This paper presents a 3D dynamic failure analysis of linear elastic body by using particle discretization scheme finite element method (PDS-FEM). PDS-FEM uses two sets of non-overlap characteristic function to discretize function and function derivative. Unlike ordinary FEM, PDS-FEM can easily calculate crack, which is the discontinuity in displacement function. The target is a thin epoxy plate with two anti-symmetric notches under uni-axial tensile boundary condition. A time depend failure criterion, called Tuler - Butcher criterion is applied. The simulation results are compared with the experimental results, which are captured by an image sensor at the rate of one million frames per second. In real world, no ideal isotropic homogeneous body exists. Disturbances exist everywhere. Crack is sensitive to local heterogeneity. Since the mesh configuration determines the candidate crack distribution in PDS-FEM, the uncertainty can be modeled by adding disturbance to the mesh configuration. By using Monte-Carlo simulation, the crack patterns observed in experiment, including bending, kinking and bifurcation are successfully simulated by using PDS-FEM.

Keywords Three dimensional dynamic simulation of fracture, stochastic model, brittle failure, photo-elastic experiment

1. Introduction

The simulation of fracture has been a challenging problem in solid continuum mechanics [1-2]. There are two difficulties in reproducing experiment results numerically: 1, accuracy and efficient numerical method is needed; 2, due to the limitation of observing technology, a stochastic model, which can represent the uncertainties, needs to be carefully designed.

For simulation of crack growth, varieties of numerical methods have been developed, such as E-FEM, X-FEM [3], discontinuous Galerkin method and meshfree methods. However, the original version of these methods has two common drawbacks: (1), the bifurcation or branching could not be calculated, which is essential for brittle materials, such as epoxy resin, rock and concrete; (2), the crack configuration is simple, normally in one dimension, so complex and detail configuration cannot be expressed. Recently, the improved version of above methods has been proposed by many researchers. The static, quasi-static and dynamic analysis can be successfully carried out [4-7].

Besides aforementioned methods, the newly developed method, called particle discretization scheme finite element method (PDS-FEM) is another candidate [8], for its numerical efficiency and capability of calculating bifurcation. In order to verify the accuracy and numerically efficiency of this method, a thin epoxy resin plate with two notches located anti-symmetrically in the middle under uni-axial tensile has been carried out numerically and experimentally. The quasi-static state of PDS-FEM has been developed by Oguni et al [9]. The comparison results show similarity between the simulation and experiment results.

In order to study the dynamic crack growth, we extend PDS-FEM to dynamic state [10]. PDS-FEM is originally formulated for Lagrangean at quasi-static state, and hence the extension to dynamic state is straightforward. Special attentions, however, have to be paid to time integration since

cracking releases strain energy and changes stiffness matrix drastically. High robustness is required for the time integration, and we adopt Hamiltonian formulation so that most robust algorithm which is proposed in the field of computational quantum mechanics can be employed for the time integration.

In real world, there is no ideal isotropic homogeneous body. Various kinds of disturbances exist everywhere. Due to limitation of the observation technology, the material property and boundary condition can hardly measure accurately. The difference between numerical setting and reality is called disturbance. Since crack is sensitive to local heterogeneity, even with the same setting, the crack paths of experimental samples are still somehow different from each other. In this paper, the authors try to reproduce a fracture experiment of a thin epoxy resin plate. In order to model the heterogeneity, a stochastic model is proposed, which introduces certain perturbation to the homogeneous body. Then, a Monte-Carlo simulation is carried out, from which, the crack patterns observed from corresponding experiments are successfully simulated.

The content of the present paper is as follows: section 2 briefly explains the extension of PDS-FEM to dynamic state. We formulate the dynamic extension of PDS-FEM by using discretized Hamiltonian, so that a robust algorithm can be applied to the time integration. Section 3 is devoted to discuss modeling of weak heterogeneity. The modeling is made by using different candidates of possible crack extensions, which is realized by using different meshes. Section 4 contains a Monte-Carlo simulation for a thin epoxy resin plate with a pair of anti-symmetric notches located in the middle. Also, the simulation results are compared with corresponding experiments, which are captured by a high frequency image sensor at the rate of 1 million frames per second. Concluding remarks are pointed out in section 5.

2. Extension of PDS-FEM to dynamic state

On the viewpoint of the numerical computation, it is not easy to analyze the crack growth, since cracking not only releases strain energy, but also changes the stiffness matrix. A robust algorithm that can handle such a change is required. The algorithm is also required to guarantee symplecticity, i.e., the total energy and momentum should be conserved during the crack growth.

A robust algorithm of time integration has been studied in the field of computational quantum mechanics [11]. To implement such an algorithm, we formulate the dynamic extension of PDS-FEM using Hamiltonian. We start from the following Lagrangean of a linearly and isotropically elastic solid, denoted by B, with elasticity $\mathbf{c}$, density ρ, displacement $\mathbf{u}$, stress $\boldsymbol{\sigma}$ and strain $\boldsymbol{\varepsilon}$:

$$L[\mathbf{u},\dot{\mathbf{u}};\boldsymbol{\varepsilon},\boldsymbol{\sigma}]=\int_B \frac{1}{2}\boldsymbol{\varepsilon}:\mathbf{c}:\boldsymbol{\varepsilon}-\frac{1}{2}\rho\dot{\mathbf{u}}\cdot\dot{\mathbf{u}}+\boldsymbol{\sigma}:(\nabla\otimes\mathbf{u}-\boldsymbol{\varepsilon})\,dv\,. \tag{1}$$

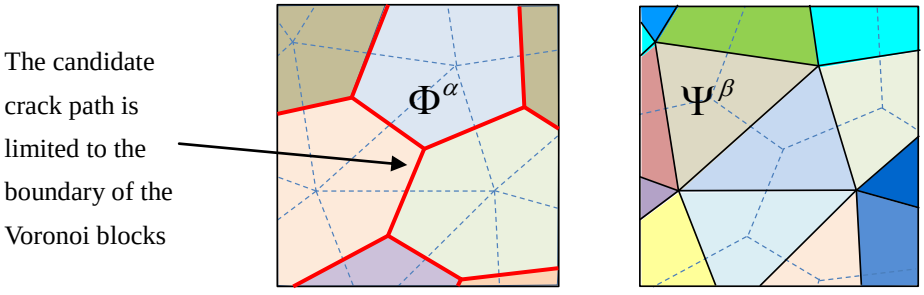

Figure 1. Two dimension decomposition by using particle discretization scheme

The discretization is made by using dual Voronoi $\{\Phi^{\alpha}\}$ and Delaunay tessellations $\{\Psi^{\beta}\}$, and their characteristic functions $\{\phi^{\alpha}\}$ and $\{\psi^{\beta}\}$ are used as basis functions. Note that, the displacement is discretized by Voronoi tessellations, while strain and stress are discretized by Delaunay tessellations:

$$\begin{aligned} u(x,t) &= \sum_{\alpha} u^{\alpha}(t)\phi^{\alpha}(x), \\ (\varepsilon,\sigma)(x,t) &= \sum_{\beta} \left(\varepsilon^{\beta},\sigma^{\beta}\right)(t)\psi^{\beta}(x). \end{aligned} \tag{2}$$

The following discretized wave equation is derived from L and the discretized functions:

$$M^{\alpha}\ddot{\mathbf{u}}^{\alpha}(t) + \sum_{\alpha'} \mathbf{K}^{\alpha\alpha'} \cdot u^{\alpha'}(t) = 0, \tag{3}$$

where M^{α} is the mass of the α^{th} Voronoi tessellation, the superscript α' stands for the α'^{th} adjacent Voronoi tessellation. Note that $\mathbf{K}^{\alpha\alpha'}$ is the stiffness matrix of PDS-FEM. This $\mathbf{K}^{\alpha\alpha'}$ coincides with an element stiffness matrix of FEM with linear tetrahedron elements [8]. Also, it should be noted that Eqn. 3 automatically leads to a lumped mass matrix. No approximation is needed to derive the lumped mass matrix, unlike ordinary FEM. This is the advantage of PDS-FEM, since, as shown in Eqn. 3, displacement is discretized as a set of rigid body displacement, or a continuum is regarded as an assembly of rigid body particles.

From this discretized wave equation, a discretized Hamiltonian of the following form is defined:

$$H = \sum \frac{1}{2}\mathbf{q}^{\alpha} \cdot \mathbf{K}^{\alpha\alpha'} \cdot \mathbf{q}^{\alpha} + \frac{1}{2\mathbf{M}^{\alpha}}\mathbf{p}^{\alpha} \cdot \mathbf{p}^{\alpha}, \tag{4}$$

where $\mathbf{p}^{\alpha} = \dfrac{\partial L}{\partial \dot{\mathbf{u}}^{\alpha}}$ and $\mathbf{q}^{\alpha} = \mathbf{u}^{\alpha}$ are the momentum and displacement of the α^{th} Voronoi tessellation.

We take advantage of the bilateral symplectic algorithm [12] as a robust algorithm of the time integration of Eqn. 4. The main advantage of this algorithm is that in order to achieve the accuracy of the order of Δt^N with Δt and N being time increment and an integer, it needs $2N$ times iteration for the interval of $2\Delta t$. Until now the highest order derived for this algorithm are four. In this paper, the fourth order is used.

3. Modeling of weakly heterogeneity for cracking

For brittle materials, it is usually observed that a crack propagates in an unpredictable manner, when subjected to dynamic loading. For instance, kinking and brunching are induced during the process of crack growth, or shattering due to multiple cracking is observed at high loading rate.

The key task of this paper is a numerical experiment that uses a set of weakly heterogeneous bodies. In the numerical model, several parameters, such as failure criteria, material properties, flaws' positions, can hardly be obtained accurately. However, it is not necessary at all to make all these parameters to be the stochastic variables, we can assign only a few to be stochastic variables, and others can be assigned as constants according to experience for simplicity. In this way, all the variability of unknown parameters can be represented by the designed stochastic variables.

Generally speaking, two methods can be used to model heterogeneity, adding perturbation to material properties of either deformation or fracture. PDS-FEM takes a simple treatment of weak heterogeneity, as: material properties are uniform except for a parameter for fracture, and cracking are allowed only on some of predetermined weak plane segments.

PDS-FEM uses a boundary facet as a set of pre-determined weak plane segments for possible crack extensions. The location of the weak plane is pre-determined by mesh configuration. In order to model the weak heterogeneity, we add disturbance to the location of mesh mother points, from which, a lot of samples with slightly different fracture property can be generated. However, there are two difficulties in this method: generating unbiased distribution may result in ill-shaped Delaunay elements, i.e., some elements with large aspect ratio; a simple solution of forcing the aspect ratio of the Delaunay elements in a certain range leads to biased distribution of some clusters of Voronoi mother points. The unbiased distribution of the Voronoi mother points and the aspect ratio control of the Delaunay elements are in a trade-off relation. As a compromise, we start from one distribution of the Voronoi mother points with majority of the Delaunay elements being well shaped, and modify this distribution randomly to generate other distributions without changing the geometry of the target model.

The mesh size is regarded as a parameter which represents the degree of material heterogeneity; the size becomes smaller as the distribution of material parameters is closer to being uniform. For designing the stochastic model of a real experiment, we need to identify the degree of material heterogeneity or the mesh size. However, with limited observation equipment, the degree of heterogeneity of real samples cannot be measured easily. Therefore, the authors try to start from a standard mesh configuration, which takes a balance between the accuracy and computation overload. If the crack path solutions of the numerical experiments show that the variability is not large enough to include the experimental results, then we have to find ways to increase the degree of heterogeneity in the stochastic model: (1), apply larger mesh size, while ensuring the required accuracy; (2), add additional perturbation to material properties of deformation. Thus, in the numerical experiment presented in section 4, we start from a standard mesh configuration as this: finer meshing is used near the crack tip, to allow a wider choice of crack extension, while meshing becomes coarser farther from the crack tip to save computation overload.

4. Monte-Carlo simulation of crack propagation

This section carries out a numerical experiment of executing Monte-Carlo simulation of heterogeneous samples, in order to reproduce the real experiments' phenomena.

4.1. Problem setting

We study a thin plate of 5×24.5×140 mm, which includes two anti-symmetric parallel notches of height 0.6 mm; see Fig. 2. It is assumed that the material is linearly elastic; see Table 1. For dynamic analysis of brittle material we need to consider the time effect, since dynamic fracture is a time-dependent phenomenon [13-14] which depends on the stress pulse duration, also from experiment study, it is observed that, the material strength is higher than static strength for high loading rate [15-16]. Concerning about this, a time dependent material strength failure criterion called Tuler Butcher criterion [17] is adopted in this paper:

$$\int_0^{\tau_f} \left(\sigma_1 - \sigma_0\right)^{\beta} dt \geq K_f , \tag{5}$$

for $\sigma_1 \geqq \sigma_0 \geqq 0$, where σ_0 and σ_1 are a threshold stress and the maximum stress, τ_f is fracture duration and K_f is the stress impulse for failure. This criterion means that a crack grows if accumulated stress in fracture duration reaches a critical value. It is assumed that $\beta = 2$ and $K_f = 10^{-8}$, σ_0 is equal to the static tensile strength, and τ_f is assigned to be the time step used in time integration; these parameters should be calibrated according to experimental data, which are not

available at this moment. However, as mentioned above, the variability of the parameters can be presented by the disturbance in mesh configuration.

Table 1. Material properties of epoxy resin

Young's modulus (Mpa)	3300
Poisson's ratio	0.38
Tensile strength (Mpa)	35.0
Epoxy density (kg/m^3)	1180

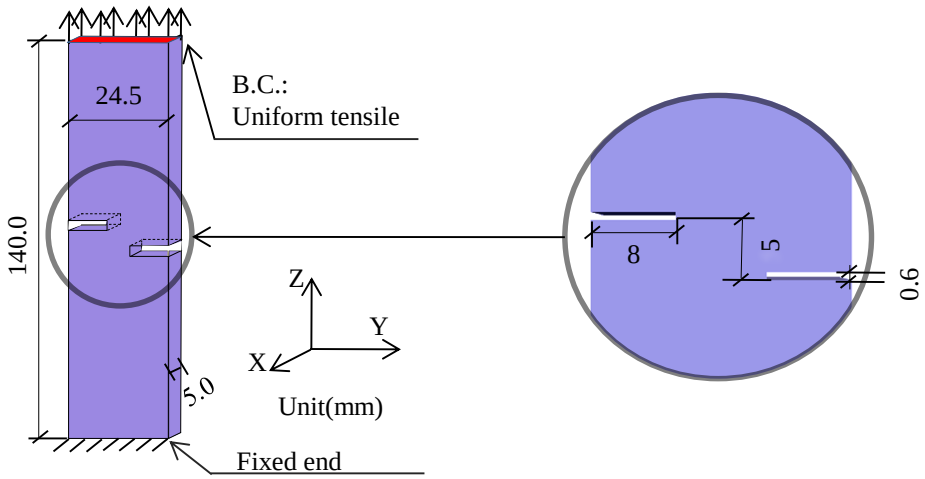

Figure 2. Analysis model

The force boundary condition is posed. The bottom end of the model is fixed, and the top end is pulled up in longitudinal direction. The loading rate is set to be 5N/s. Since the loading rate is small, the initial load of simulation is set to be 135N to save computation time. No element failure exists under this initial load. Following the PDS-FEM discretization, the crack tip is modeled as a notch with 0.6 mm height; the vertical surface of the notch is discretized by using 2 elements. The average mesh size is 1.0 mm at the top and bottom surfaces of the model to save computational overload. The time increment is set to be $\Delta t = 5.0 \times 10^{-9}$s.

200 samples with slightly different mesh configurations or distributions of candidate crack path for PDS-FEM are prepared for Monte-Carlo simulation. The number of samples is decided by checking the convergence of average crack path position through the specified cross-sections.

4.2. Simulation results and experimental comparison

For numerical simulation, the crack patterns can be classified into two groups: (1), the crack paths are symmetrically distributed; (2), one crack is fully developed horizontally from either of the notches. Fig. 3 shows eight typical crack path solutions of the model with small heterogeneity. Bifurcation is also observed in the simulation results; see Fig. 3.5~Fig.3.8.

In order to record the development of crack growth and stress changes of the epoxy resin thin plate, an ultra high speed video camera, which can capture images at the rate of 1 million frames per second, is used herein [18]. The photo-elastic technology [19] is used to show the stress distribution of experimental samples. Fig. 4 shows the final stages of four typical photo-elastic fringe patterns.

Within 16 samples, no sample with perfect anti-symmetric distribution of the two crack paths has been found. This is because the number of experimental samples is too few to include a sample with sufficiently homogenous material property and symmetrical boundary condition at the same time. The typical crack patterns can be classified into two groups: (1), one main crack path develops from either one of the two notches; (2), the two crack paths are more or less anti-symmetrically distributed. From experiments, some cracks bifurcate at the end of experiments.

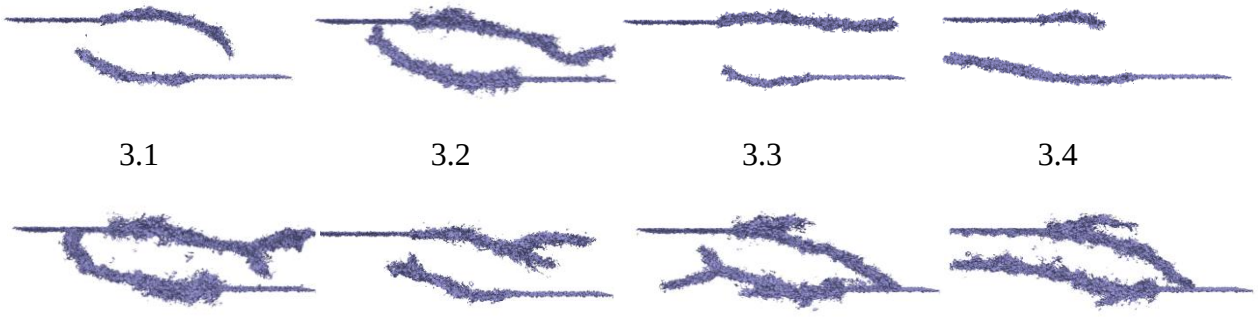

3.1 3.2 3.3 3.4

3.5 3.6 3.7 3.8

Figure 3. The typical crack paths projection into YZ plane
under force boundary condition of loading rate 5N/s

Among 200 numerical samples, we find the samples, whose crack paths coincide with experimental results. In order to make further comparison between the simulation results and experimental results, the stress distribution of simulation has been converted into photo elastic fringe patterns. Fig. 5 and 6 shows the experimental photo-elastic fringe patterns and the numerically synthesized fringe patterns. From these comparisons, the crack growth processes of these two samples are successfully simulated by the method proposed in this paper.

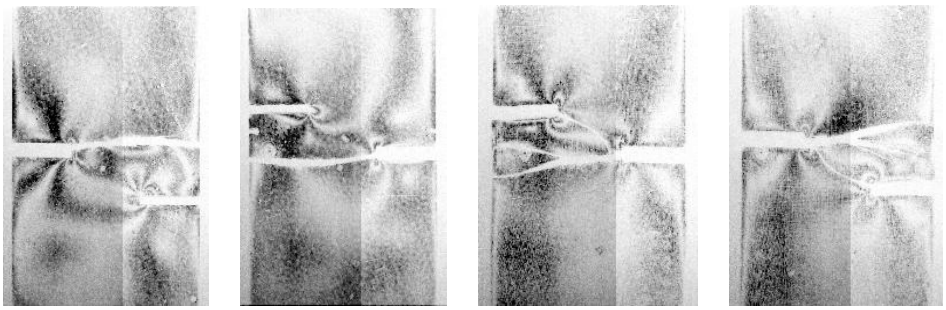

4.1 4.2 4.3 4.4

Figure 4. Photo elastic frames of experiments' final stages, $t = 100\mu s$ (with colors reversed)

Experiments

$t = 40\mu s$ $t = 70\mu s$ $t = 100\mu s$

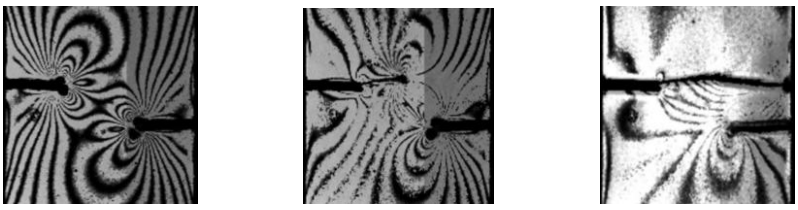

(a), fringe patterns of experimental sample 4.1

Simulations

$t_0 = 76,179,191\mu s$ $t = t_0 + 40\mu s$ $t = t_0 + 70\mu s$ $t = t_0 + 100\mu s$

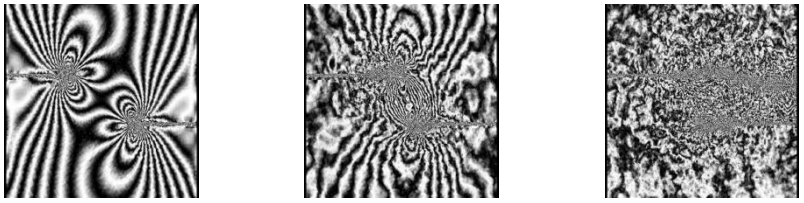

(b), synthesized fringe patterns of numerical sample 3.3

(c), crack growth process of numerical sample 3.3

Figure 5. One main crack path

Experiments

$t = 30\mu s$ $t = 50\mu s$ $t = 70\mu s$

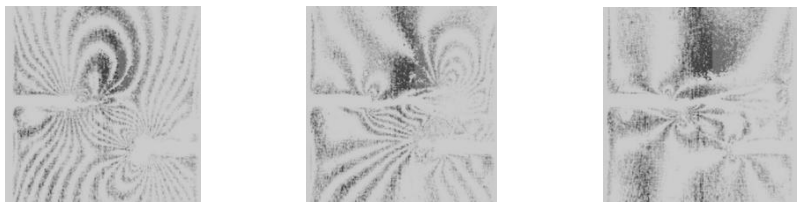

(a), fringe patterns of experimental sample 4.4

Simulations

$t_0 = 76,179,191\mu s$ $t = t_0 + 30\mu s$ $t = t_0 + 50\mu s$ $t = t_0 + 70\mu s$

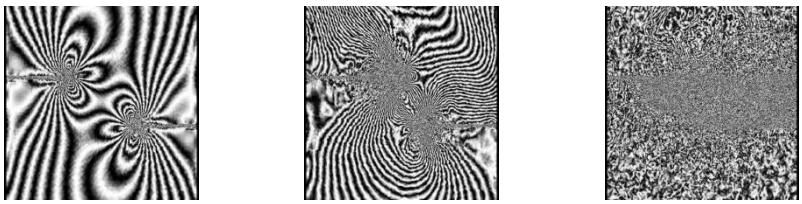

(b), synthesized fringe patterns of numerical sample 3.6

(c), crack growth process of numerical sample 3.6

Figure 6. Bifurcation

(The colour of all images in Fig. 6.a and b has been reversed, since the records are too dark to see.)

Before crack starts, the experimental fringe patterns and simulation results show significant similarity. However, when crack develops, the stress distribution of the simulation becomes blurred. There are three possible reasons for this:

(1) The mesh density is not large enough near the crack tips. In the simulation, the element size is still large, so the energy of the stress wave released from broken elements is significant. On the contrary, the granularity of the epoxy resin is small, and the energy released from the broken of crystalline grain is small and continuous in real experiments.

(2) Friction, thermal as well as acoustic energy consumption mechanics due to cracking have not been considered in this simulation. The released strain energy blurs the simulated photo-elastic fringe patterns.
(3) Ductile fracture may happen in the experiments under indoor temperature.

5. Conclusion

There is no ideal homogeneous body in the world. In order to model the heterogeneity, PDS-FEM offers a nature way by adding disturbance in the mesh configuration. This paper conducts a tensile fracture experiment of a thin epoxy resin, and builds a stochastic model with the distribution of candidate crack path set as stochastic variables. Monte-Carlo simulation is carried out. With specified basic mesh configuration, the simulation results reproduce the crack growth of corresponding experiments, including bending, kinking and bifurcation. The heterogeneity is successfully modeled.

Before crack develops, the stress distribution of simulation shows great similarity with experimental photo-elastic fringe patterns captured by a high speed camera. When crack begins, the fringe patterns of simulation become blurred. Three possible reasons have been proposed and more realistic problem setting is needed to increase the similarity between the results of simulation and experiment in future study.

Acknowledgements

This research is partially supported by the Central Public-interest Scientific Institution Basal Research Fund of China (Grant No. 2011B-05), China postdoctoral Science Foundation, and Natural Science Foundation of Hei Longjiang Province of China (Grant No. LC2012C32). These supports are greatly appreciated.

References

[1] J. Oliver, Modelling strong discontinuities in solid mechanics via strain softening constitutive equations. Part 2: Numerical simulation. *Int. J. Num. Meth. Eng*., 39(21), (1996) 3601-3623.
[2] N. Moes, J. Dolbow, T. Belytschko, A finite element method for crack growth without remeshing. Int. J. Num. Meth. Eng., Vol. 46:1, (1999) 131–150.
[3] J. Oliver, A. Huespe, and P. Sanchez, A comparative study on finite elements for capturing strong discontinuities: E-FEM vs X-FEM. Computer methods in applied mechanics and engineering, 195(37), (2006) 4732-4752.
[4] T. Rabczuk, S. Bordas, and G. Zi, A three-dimensional meshfree method for continuous multiple-crack initiation, propagation and junction in statics and dynamics. Comput. Mech., 40(3), (2007) 473-495.
[5] S. Bordas, T. Rabczuk, and G. Zi, Three-dimensional crack initiation, propagation, branching and junction in non-linear materials by an extended meshfree method without asymptotic enrichment. Eng. Fract. Mech., 75(5), (2008) 943-960.
[6] F. Stan, Discontinuous Galerkin method for interface crack propagation. Int. J. Mater. Forming 1, (2008) 1127-1130.
[7] N. Sukumar, B. Moran, T. Black, and T. Belytschko, An element-free Galerkin method for three-dimensional fracture mechanics. Comput. Mech., 20(1), (1997) 170-175.
[8] M. Hori, K. Oguni, and H. Sakaguchi, Proposal of FEM implemented with particle discretization for analysis of failure phenomena. J. Mech. Phys. Solids: 53(3), (2005) 681-703.

[9] K. Oguni, L. Wijerathne, T. Okinaka and M. Hori, Crack propagation analysis using PDS-FEM and comparison with fracture experiment. Mech. Mater. Phys. Solid, 41(11), (2009) 1242-1252.
[10] H. Chen, L. Wijrathne, M. Hori, and T. Ichimura, Stability analysis of dynamic crack growth using PDS-FEM. Struct. Eng. Earthq. Eng., 29(1), (2012) 1s-8s.
[11] M. West, Variational integrators, California Institute of Technology, 2004.
[12] L. Casett, Efficient symplectic algorithms for numerical simulations of Hamiltonian flows. Phys. Scripta, 51, (1995) 29-34.
[13] T. Nojima, T. Crack stability in rate sensitive ceramics and their rate dependence. J. Phys. IV:4, (1994) C8-689-C8-694
[14] A. Nyoungue, Z. Azari, M. Abbadi, S. Dominiak, and S. Hanim, Glass damage by impact spallation. Mater. Sci. Eng.: A, 407(1), (2005) 256-264.
[15] J. Jeong, H. Adib, and G. Pluvinage, Proposal of new damage model for thermal shock based on dynamic fracture on the brittle materials. J. Non-cryst. Solids, 351(24), (2005) 2065-2075.
[16] Y. Xia, X. Wang and B. Yang, Brittle-ductile-brittle transition of glass fibre-reinforced epoxy under tensile impact. J. Mater. Sci. Lett., 12(18), (1993) 1481-1484
[17] B.M. Butcher, L.M. Barker, D.E. Munson and C.D. Lundergan. Influence of Stress History on Time-dependant Spall in Metals. AIAA, Vol. 2:6, (1964) 977-990.
[18] T.G. Etoh, D. Poggemann, G. Kreider, et al. An image sensor which captures 100 consecutive frames at 1000000 frames/s. Electron Devices, IEEE Transactions on, 50(1), (2003) 144-151.
[19] M. Wijerathne, K. Oguni, and M. Hori, Inverse analysis method for photoelastic measurement of 3D stress state. Key Engng. Mater., Vol. 261, (2004) 753–758.